Proceedings of the 2nd International Conference on Green Energy, Environment and Sustainable Development (GEESD2021), D. Dobrotă and C. Cheng (Eds.)

doi:10.3233/ATDE210286

Research and Application of the 3D Model of Beijing in Urban Planning Based on Oblique Photogrammetry

Yanzhi SUN[a,1], Xi WEI[b] and Tongsheng ZHANG[a]
[a] *China Urban Construction Design & Research Institute Co. Ltd., Beijing 100120, China*
[b] *China Academic of Electronics and Information Technology, Beijing 100041, China*

Abstract. In recent years, with the accelerated development of the urbanization and the continuous emergence of the smart cities, the new requirements and the challenges have been raised for the urban governance and the urban planning. Based on the oblique aerial photogrammetry technology and the 3D automatic modelling technology, this study constructs the high-precision basic data of the 3D urban model of Beijing and verifies the 3D model's precision comprehensively by using two verification methods: the point accuracy assessment and the plane accuracy assessment. And then, using the validated 3D model data and taking the demolition of the illegal buildings in urban planning as an example, an application of the 3D model is studied in the simulated environmental scenes of the urban planning, which also provides a reference for the development of the smart cities in the future.

Keywords. Urban planning, oblique photogrammetry, 3D automatic modelling technology

1. Introduction

The urban was a symbol of the human civilization, which was also the product of the economic development at a certain stage. In recent years, with the continuous acceleration of the urbanization, the problems and the challenges were increasingly prominent and severe in the urban environment, the resources and the management. What's more, the contradiction between the increasing scale of the people's demand and the limited urban supply would also increase continually. The further development of the urban needed to explore some new paths [1]. With the advancement of the internet technology, the 3D simulation technology and the smart urban, the traditional geographic information technology had been injected with the fresh vitality and the 3D GIS loaded on the internet was developing towards the digitalization and the intelligence [2]. Due to being lack of the complete dimension information, the traditional 2D GIS could not reflect all the reality information of the urban space. However, the 3D geographic information system could provide the whole texture map data and had the characteristic of the spatial analysis function and the strong 3D visualization expression [3]. Moreover, the 3D model had the advantages of being

[1] Corresponding Author, Yanzhi SUN, China Urban Construction Design & Research Institute Co. Ltd., Beijing 100120, China; Email: sunyz.12s@igsnrr.ac.cn.

modelled more effectively, less cost and so on, which was particularly suitable for the application of the urban information displaying, the emergency management, the intelligent transportation, the public security and other public managements [4]. Different from lidar laser point cloud model, the 3D real scene model has the better texture representation and the more realistic feature representation than the lidar laser point cloud model. In addition, the acquisition cost of the 3D real scene model is lower than that of the Lidar data. In view of the present problems in the process of the urban development, it was needed to supplement the auxiliary analysis of the 3D geographic information and develop the decision-making platform system, which integrated all kinds of information with the 3D space information. By monitoring the various urban resources in space distribution and real-time operation, the inner links between them were analysed to configurate and schedule the resources reasonably. Then the rapid response and the coordination of each department processing urban were improved obviously.

This research used a big plane carrying the five oblique cameras and other posture and position fixing devices to obtain the five different angles (down, forward, backward, left, right) ground images, the pictures gesture and the flight height. The 3D model was built through the data import, the aerial triangulation solution, the irregular triangle net construction and the automatic texture mapping process. The point positional accuracy and the plane precision evaluation methodology were used to evaluate and validate the model data quality. The model data was taken as the based map application data and the 3D urban public management integrating system was built as the based platform. Moreover, the illegal building demolition was taken as the typical application case, so the "platform + business system" mode was formed for the urban planning work. The large-scale 3D scene fast visual expression and the huge amounts of 3D data intelligent analysis were realized to provide the comprehensive public management service for the urban construction. In addition, all kinds of urban business applications were supported to be developed smoothly and it played an important role in the construction of the harmonious society and the public safety. What's more, it laid a foundation for the construction of the smart cities [5]. The overall technical roadmap of the study was shown in figure 1 as below.

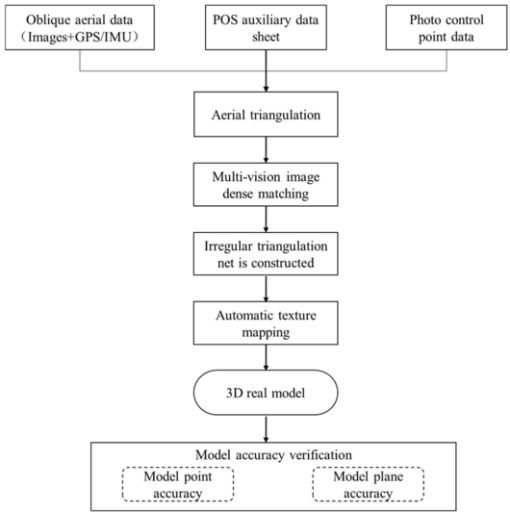

Figure 1. The general technical route.

2. The Construction of the Urban 3D Model

The 3D model data was built based on the oblique aviation image data sources. The oblique image data was configurated with the vertical image data to a unified operating system. And then the 3D modelling environment was needed to be built from multiple visual angles to form the precise reconstruction under the strict imaging relations, which could make up for the limitations of one single data source perspective, the resolution, the object occlusion and so on. By the integrating modelling environment, the accuracy and efficiency were increased greatly. The combined data source of the oblique photography could overcome the differences in the aspect of the image resolution, the photography angle, and the image radiation characteristics and so on. Moreover, by the comprehensive applications of the POS assistance data, the DSM guidance and so on, the high-precision 3D modelling was highly automated.

Firstly, the combined adjustment of the regional network was carried out by the beam method and the triangulation relationships between the multi-view oblique images established by the aerial triangulation were generated into a Triangulated Irregular Network (TIN). Then the TIN was used to generate the 3D white model. Finally, the image texture was mapped to the white model by the automatic texture mapping technology to obtain the 3D model.

2.1. The Oblique Aerial Photogrammetric Data Acquisition

The oblique aerial photography was a new kind of aerial photography which used the oblique aerial photogrammetry to obtain the ground object information. It was different from the traditional vertical aerial photography and described as follows. The five oblique aviation cameras were carried on the air vehicle platform and the intelligent flight control system was applied to realize automatic cruise. At the same time, the five direction image data was obtained and it was needed to cooperate with the IMU (Inertial Measurement Unit) and GPS (Global Positioning System) to obtain the high precision of the position and the posture information. Through the specific data processing software for the data processing, all of the images were unified to a unified coordinate system. Meanwhile, the professional flight control team carried out the topographic survey, the aerial point calculation, the aerial path planning, and the optical camera parameter adjustment operation and so on to ensure that the aerial photography data was qualified.

2.2. Multi-angle Aerial Triangulation

The multi-angle image data included the vertical aerial image and the oblique aerial image data. The POS data obtained from the aerial photographic was taken as the initial exterior orientation elements of the multiple perspective aerial images. Afterwards the space coordinates of each pixel in the image were calculated by combining with the sensor-imaging model. A large number of connections between images were generated by using the multiple baseline characteristics matching technology. Then the angle joint aerial triangulation was realized by combining with a small amount of the field control points through the regional net adjustment.

2.3. Irregular Triangulation Net (TIN) Construction

The stereopair were created based on the images after distortion correcting and the high-precision exterior orientation primitives after aerial triangulation optimizing. Moreover, the multi-element and the multi-visual image matching technology were adopted based on the space plane of the rules grid partition. By integrating the image feature points with the object surface element and making full use of the feature information of the multi-visual image and the imaging information, the matching strategy of the reference image unfixing was used and the multi-visual images were matched densely. The redundant information of the multi-visual matching was effectively used to avoid the impact that the occlusion made on matching. In addition, the parallel algorithm was used in order to improve the calculation efficiency and the same points coordinates of the multi-visual image were obtained quickly and accurately. Then, the high-density 3D point cloud data of the ground object was obtained and the TIN model with different levels of detail (LOD) was constructed by the point cloud data. Through the optimization of the triangulation network, the size of the internal triangulation was adjusted to the proportion matching the original image resolution. Meanwhile, through the analysis of the continuous surface change, the triangulation networks in relatively flat areas were simplified to reduce data redundancy and the vector architecture of the urban 3D TIN model was obtained as figure 2.

Figure 2. The irregular triangulation net.

2.4. Automatic Texture Mapping

The realization of the texture association of the 3D TIN model included the registration between the 3D TIN model and the texture image. Because the images obtained from the oblique photography were the multi-angle, the same object appeared on multiple images. It was very important to choose the most suitable target images. The normal equation of each triangle of the model surface and the angle relationship among the 2D images were adopted for the triangular mesh model to measure the appropriate texture images. The smaller the angle was, the more the image plane and the triangle were closed to parallel and the higher the texture quality was. Based on this method, each triangle of the three-dimensional TIN model only corresponded to one target image.

Then the geometric relationships between each triangle of the 3D TIN model and the corresponding regions in the image were calculated and the corresponding actual texture regions of each triangle face were found in the texture image. Finally, the registration of the 3D TIN model and the texture images was realized. The registered texture images were back projected onto the corresponding triangular surfaces so as to render the model realistically at any time and the texture attachment was realized as figures 3 and 4.

Figure 3. The 3D white model.

Figure 4. The texture mapping to construct 3D real model.

3. Test and Accuracy Analysis

3.1. The Test Validation

The large overlap design scheme was adopted in the image overlap degree of the oblique aerial photogrammetry data, which took the smallest image covering the ground as the standard. The directional overlap rate of the adjacent images was guaranteed to be better than 70%, so was the lateral overlap rate. The downward-looking resolution was 0.05 m. Moreover, it was needed to ensure that there was no obvious colour bias in the imaging of each camera and obvious colour bias difference between different cameras. The tonal of the photographed data should be consistent. Figure 5 showed the schematic diagram of the oblique photogrammetry image data obtained from the multiple perspectives.

3.2. Model Accuracy Analysis and Verification

Through the intuitive 3D real model data obtained above, the 3D geographic coordinate information of the required point position could be obtained directly from the 3D model. And the actual distance between points and the practical area of the selected area could also be directly measured from the 3D model. Many spatial analysis functions such as visibility analysis, slope analysis and submergence analysis were developed and applied based on the 3D real model [6]. For the actual ground objects, the 3D real model data was generally not determinable. There were some factors that affected the model precision such as the acquisition of the original data, the oblique data and the preprocessing of the auxiliary data, the construction stage of the 3D real model and so on. In order to apply the 3D real model data to the urban planning, the

evaluation indexes were needed to evaluate and verify the model accuracy. However, so far there was no general and mature method and evaluation system to verify the 3D real model. Therefore, the accuracy of the model was verified from the perspective of experimental analysis, which was of great significance for the correctness and practicability of the 3D real model [7]. In this study, the point accuracy analysis and the plane accuracy analysis methods were synergistically used to evaluate the quality of the obtained 3D real scene model quantitatively.

Figure 5. The schematic diagram of five perspectives of the same ground object.

3.2.1. Point Accuracy Analysis and Verification

In the actual measurement, the commonly used method to verify the data accuracy was to compare the high-precision instrument measurement results with the measurement results. And the same method could be also applied to the evaluation of the image data quality of the oblique photogrammetry [8-9]. The specific method was shown as follows. Firstly, the 20 feature points were extracted from the oblique 3D model and their coordinates were recorded in the 3D spatial coordinate system (x, y, z). The high-precision network RTK was used to measure and record the WGS-84 coordinate system, the ellipsoidal height and the 3D coordinates (x, y, z) of the same 20 feature points in the experimental area, so as to verify the accuracy of the obtained oblique 3D real scene model with reference data. Secondly, it was needed to calculate the differences between the coordinates of the oblique 3D model and the network RTK measurement reference coordinates to get the values of Δx, Δy and Δz respectively. As shown in figure 6, it was different between the coordinates of the oblique 3D model and the measured reference coordinate of the network RTK. As can be seen from figure 6, the elevation coordinate differences were mostly negative and the maximum value of the Δx was at point 5. Moreover, the minimum value appeared at point 6. In addition, the maximum value of the Δy was at the point 5 and the minimum value appeared at

the point 20. The maximum of the Δz was at point 9 and the minimum was at point 1. In general, the coordinate differences were concentrated in negative values. The mean values of Δx, Δy and Δz was 0.00112, -0.01335 and -0.02283 respectively. It could be concluded from the analysis in figure 6 that the observed values of the Δy changed relatively stable with relatively small errors, while the value of the Δz presented relatively large errors. The reason for this may be that there were many redundant point clouds on the oblique 3D model, which resulted in the lack of accuracy in point selection.

Figure 6. The coordinate difference between oblique photogrammetry and RTK measurement.

Taking N as the number of all points, where N=20. Based on this calculation, the axial errors and point median errors of each coordinate point were shown as follows.

$$\delta_x = \pm\sqrt{\frac{\sum_{i=1}^{N}\Delta x_i^{\,2}}{N}} = \pm 0.07552 \tag{1}$$

$$\delta_y = \pm\sqrt{\frac{\sum_{i=1}^{N}\Delta y_i^{\,2}}{N}} = \pm 0.04332 \tag{2}$$

$$\delta_z = \pm\sqrt{\frac{\sum_{i=1}^{N}\Delta z_i^{\,2}}{N}} = \pm 0.07371 \tag{3}$$

$$\delta_{xy} = \pm\sqrt{\delta_x^2 + \delta_y^2} = \pm 0.08706 \tag{4}$$

According to the above equations, the median error of the 20 feature points in the experimental area was 0.07552 m in the X-axis direction, 0.04332 m in the Y-axis direction, 0.07371 m in the z-axis direction and 0.08706 m in the plane elevation

direction. It could be concluded that the errors of both the elevation and the plane were less than 10 cm (two pixels). It could be seen from the comparison in table 1 that the accuracy could meet the accuracy of 1:2000 and 1:5000 scale topographic maps and the verification results of the point accuracy could meet the application requirements of the 3D models [10-11].

Table 1. Scale accuracy.

Scale	1:500	1:1000	1:2000	1:5000	1:10000
Scale accuracy	0.05	0.10	0.20	0.50	1.00

3.2.2. Plane Accuracy Analysis and Verification

To further validate the plane precision of the 3D model, it was necessary to use the multiple planar sampling points to do the surface fitting. According to the 20 feature points' coordinates selected from the 3D real model, the same points' coordinates were selected by using the high-precision GPS-RTK equipment as the reference data. Then the reference plane equation was fitted out and the selected 20 points' distances to the plane were finally calculated, which were used to validate the precision of the 3D model. In the actual measurement operation, the errors would be inevitably generated and transmitted to the subsequent data processing. A small number of points were selected for the plane fitting, which could generate a large error. Therefore, in order to reduce the errors, multiple sets of the observation data could be used to control the fitting errors. In the first place, the $P_i = (X_i, Y_i, Z_i)$, (I =1,2,3..., 20) was set as the data of the 20 points on the plane and the plane equation was solved as ax+ by+ cz =1. In the second place, it was supposed that the equation coefficient matrix composed by the 20 groups of the known point position data was as follows.

$$G = \begin{bmatrix} x_1 & y_1 & z_1 \\ x_2 & y_2 & z_2 \\ \vdots & \vdots & \vdots \\ x_N & y_N & z_N \end{bmatrix} \tag{5}$$

And then the unknown parameter matrix was set as $k = [\mathrm{a} \quad \mathrm{b} \quad \mathrm{c}]^T$. If $h = [1 \quad \cdots \quad 1]^T$, the system of equations could be constituted as $Gk = h$. According to the nature of the adjustment, the equations could not directly get the unknown parameters k. So the transposed matrix G^T was multiplied on the left in the both sides of the equations, the equations was obtained as follow.

$$G^T G k = G^T h \tag{6}$$

According to the least square principle, the equations was obtained as follow.

$$k = \left(G^T G\right)^{-1} G^T h \tag{7}$$

The plane equation of the reference plane obtained through the above calculation was as follow.

$$\mathbf{2.184 \times 10^{-7}}\boldsymbol{x} + \mathbf{4.85 \times 10^{-8}}\boldsymbol{y} + \mathbf{6.79 \times 10^{-6}}\boldsymbol{z} = \mathbf{1} \tag{8}$$

The distance d_i from the oblique photogrammetric coordinate point to the fitting plane was as follow.

$$d_i = \frac{ax_i + by_i + cz_i - 1}{\sqrt{a^2 + b^2 + c^2}} \tag{9}$$

It was calculated that the maximum distance between the feature point data of the oblique 3D real model and the reference fitting plane was 42.4186 mm and the minimum value was 2.32 mm. The distribution was relatively uniform and the average distance was -0.0876 mm. The distance between the point 5 and the point 17 was relatively close and the accuracy was relatively high (figure 7).

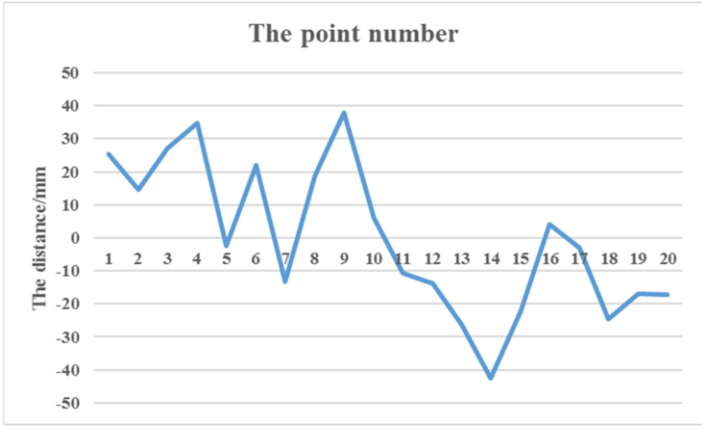

Figure 7. The distance between the oblique 3D model data and the reference fitting plane.

In order to verify the area measurement accuracy of the 3D model, six plane areas of the experimental area were selected to carry out the field measurement of the length, the width and the area with the high-precision measuring instruments and the actual area data was taken as the reference data. By using the high precision measurement function in the modelling software, the area information of the objects could be obtained from the 3D model. The data obtained from the two groups were compared and analysed as shown in the broken line diagram in figure 8. From the figure, it could be concluded that the maximum value of the area difference was 0.5 m^2, which appeared in plane No. 6. The minimum value was 0.03 m^2, which appeared in the second plane, and the errors of the other planes were all within 0.5 m^2. It could be seen that the plane accuracy of the model was high, which could be used as a reference in the subsequent urban planning application.

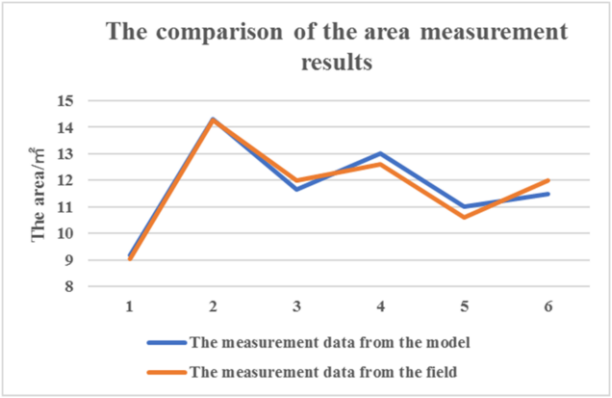

Figure 8. The comparison between model plane measurement data and field measurement data.

To sum up, through the verification methods of the point accuracy and the plane accuracy, it could be seen that the data obtained from the 3D urban model had a good precision, which could be applied to the subsequent urban planning and provided the relatively accurate data support and the reference for the governance of the urban.

4. The Application of the 3D Urban Model

Based on the above processing process and the verified 3D model, the 2D data, the business data and the multimedia data were integrated and linked to build the comprehensive platform for the urban planning and management. This study took the demolition of the illegal buildings in urban planning as an example. The urban 3D geographic data will become one of the important information of a new smart urban [12-13].

4.1. The 2D/3D Dimensional Scene Linkage Roaming

As shown in figure 9, the 2D/3D scene linkage fully made up for the deficiency of one single data browsing. On one hand, the amount of the 2D visual image data was relative less to the 3D data and the target could be quickly found on the 2D map from the wide scope. In addition, by integrating the high-precision 3D model, the geometry and the texture style of the object could be detailed observation. The object in the 3D scene could also be quickly displayed in the 2D map, so as to obtain its geographical position and surrounding features in the overall environment. The measurement function of the application system could directly obtain the dimensions and the area information of the illegal buildings in the 3D model, which could reduce the staff's work such as taking pictures, doing the field surveying and mapping at the scene to improve the work efficiency. The illegal building could be macroscopically and efficiently identified and the demolition process of the illegal building could be monitored.

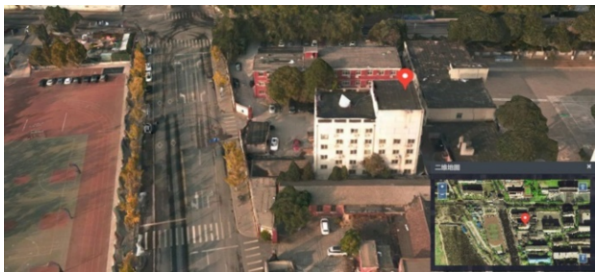

Figure 9. 2D/3D scenes linkage.

Figure 10. The point information.

4.2. Annotation Point Information Query

As to the buildings which were planning to be pulled down or the area being constructed in urban planning, the points could be marked on the 3D model and linkage with the urban information. Meanwhile, its information was updated with the progress of the work and the detailed progress and the overall deployment of the work could be managed and dispatched intuitively and macroscopically. It could provide the basic data for managers in monitoring the present situation of urban planning and deciding the major issues. The tedious works were replaced by the presentation, such as browsing a large number of documents and printing plenty of materials. At the same time, it could be also used as a 3D electronic archive file. As shown in figure 10, the point ownership information and other attribute information could clarify the division of the work in the grass-roots work, which could reduce unnecessary conflicts and ensure the smooth operation of the work.

5. Conclusion

In this study, the oblique aerial photogrammetry technology was used to efficiently obtain the multi-angle oblique image data and other auxiliary data, and the 3D model data were obtained through the combined adjustment of regional network, the aerial triangulation encryption, the TIN triangle network construction and the automatic texture mapping. The data quality of the 3D model was evaluated by using the point accuracy and the plane accuracy verification methods, which provided the reference for the application of the subsequent data in urban planning. The urban management platform was built based on the 3D data, 2D data and other data. In addition, the illegal building demolition in urban planning business was taken as an example to illustrate the application of the 3D geographic information in the actual scene. Meanwhile the whole link operation system of the oblique 3D model was also established from the data acquisition and data processing to the system platform application in urban planning. The results showed that the efficiency of the illegal building demolition work was effectively improved by using the system platform. Moreover, it integrated all kinds of information from different department and the overall progress and the detailed information of the urban were displayed by using the multimedia. It greatly assisted the managers in the perspective of the whole situation and the decision-making

of all kinds of affairs and the urban planning in the future, which played an exemplary role to the development of the smart urban.

In the future, the new smart cities will increasingly rely on the urban 3D model to establish the intelligent system based on the 3D geographic information, which can be used for the urban planning, the management, the command and the dispatching. Therefore, it can be predicted that the demand of the 3D geographic data in new smart cities will gradually become a huge market. On this basis, not only can the GIS be used by the managers in urban planning, the management, the command and the dispatching, but also can be opened to the enterprises and the public as a service, driving the development of the 3D geographic information industries in a wider application.

Acknowledgement

This research was funded by the Youth fund projects of China Construction Technology Co. Ltd., grant number Z2020Q24, the Opening project of Research Base for Beijing Studies, grant number BJXJD-KT2021-YB02, and the Innovation fund project of China Construction Technology Co. Ltd., grant number Z2019J01.

References

[1] Li J 2014 Overview on smart urban development *Journal of China Academy of Electronics and Information Technology* **9** (3) 221-225.
[2] Zhang F 2014 *Research on WebGL-Based Visualization Technologies of Large-Scale 3D Scene* (Information and Communication Engineering Graduate School of National University of Defense Technology).
[3] Cao X R, Chen X N, Yue G J, et al. 2019 Design and implementations of police emergency command system Based on 3D realistic scene *Beijing Surveying and Mapping* **33** (1) 80-83.
[4] Jiang H, Ji F and Long R 2017 The Web loading and application research of the oblique photography 3D model based on Cesium *China High-Tech* **1** (6) 3-4.
[5] Li X M, Ma Q X, Yue G J, et al. 2019 Application of 2D and 3D integrated WebGIS in urban planning *Beijing Surveying and Mapping* **33** (2) 226-231.
[6] Kobayashi Y 2006 *Photogrammetry and 3-D Urban Modelling* (School of Architecture and Landscape Architecture, Arizona State University, USA).
[7] Wang W X, Song W D and Liu Y C 2010 Precision analysis of 3D reconstruction model based on generalized stereopair *Science of Surveying and Mapping* **35** (4) 31-33.
[8] Gao S, Yuan X P and Gan S 2018 Experimental study of oblique photogrammetry in terrain 3D modeling *Journal of Henan University of Science & Technology (Natural Science)* **39** (4) 99-104.
[9] Wang B T and Wang J 2015 Production and quality analysis of 3D urban modeling using oblique photogrametric Technology *Urban Geotechnical Investigation & Surveying* (5) 80-82.
[10] Ma C L, Wang Z H, Chen J L, et al. 2008 *Specifications for Aerophotogrammetric Office Operation of 1:500 1:1000 1:2000 Topographic Maps* GB/T 7930-2008 (China Standards Press).
[11] Ma C L, Wang Z H, Xie X P, et al. 2012 *Specifications for Aerophotogrammetric Office Operation of 1:5000 1:10000 Topographic Maps* GB/T 13990-2012 (China Standards Press).
[12] Demir C and Koramaz T K 2018 GIS-based procedural modelling in contemporary urban planning practice *2018 22nd International Conference Information Visualisation (IV)* (IEEE Computer Society).
[13] Liang J M, Gong J H, Sun J, et al. 2017 A customizable framework for computing sky view factor from large-scale 3D urban models *Energy & Buildings* **149** (8) 38-44.